

Longitudinal Characteristics of Water Falling Films

Dr. Kassim Y. AL-Salman, Mohammed Kh. kadhum
Dept. of Mech. Eng./College of Engineering/University of Basrah

Abstract:

Falling liquid films have several engineering applications, and the study of these films is considered to be an important and essential aspect. This work aims to present an extensive experimental investigation and theoretical analysis to a gravity driven laminar sinusoidal falling water film over an inclined plate to study its main characteristics such as: wave profile, mean wave thickness, wavelength and wave velocity. Film characteristics were investigated for different inlet water flow rate and inclination angles to obtain the relation of the wave flow characteristics with the variables taken in the study. The results show that average wave thickness increases with Reynolds number and also with the flow direction. Good agreement was obtained between the experimental data and the theoretical results. Also, the results agreed well with the results of previous investigations.

الخلاصة:

لأغشية السوائل الساقطة تطبيقات هندسية عديدة و إن دراسة مميزات هذه الأغشية تعتبر من الأمور المهمة و الضرورية في التطبيقات العملية. تهدف هذه الدراسة إلى إجراء استقصاء تجريبي موسع وتحليل نظري على غشاء ماء طبقي ذو تموجات جيبية ساقط بتأثير الجاذبية على صفيحة لها زاوية ميلان متغيرة لدراسة المميزات الرئيسية للجريان المتموج كشكل الموجة و متوسط سمكها و طولها الموجي و سرعتها. درست مميزات الغشاء لحالات مختلفة لمعدل تدفق الماء الداخل و كذلك زوايا ميلان مختلفة لاستنتاج علاقة مميزات الجريان المتموج مع المتغيرات التي تضمنتها الدراسة. أوضحت النتائج بأن متوسط سمك الموجة يزداد مع زيادة رقم رينولدز و كذلك مع طول خط الجريان. حصل على توافق جيد بين القراءات العملية و النتائج النظرية. كذلك تتناجح هذه الدراسة اتفقت بصوره جيدة مع نتائج الدراسات السابقة.

List of symbols

Symbol	Definition	Units
a	Dimensionless film thickness, (δ/δ_0)	
b	Dimensionless local volumetric flow rate, (B/B_0)	
B	Local volumetric flow rate per unit film width over a wavelength	m^2/s
B_0	Mean volumetric flow rate per unit film width over a wavelength	m^2/s
c	Wave velocity	m/s
e_s	Rate of strain tensor	
Fr	Froude number, $(g\delta_0/U_0)^{1/2}$	
g	Gravitational acceleration	m/s^2
n_j	Unit normal vector at free surface	
\bar{p}	Pressure in liquid	N/m^2
p	Dimensionless pressure in liquid, $(\bar{p}/\rho U_0^2)$	
\bar{p}_v	Vapor pressure at free surface	N/m^2
p_v	Dimensionless vapor pressure at free surface, $(\bar{p}_v/\rho U_0^2)$	
Re	Reynolds number, $(4B_0/\nu)$	
R_1, R_2	Orthogonal radii of curvature at free surface	
t	Time	s
t_i	Unit tangential vector at free surface	
\bar{u}	Average velocity	m/s
u	Axial velocity in x-direction	m/s
u_0	Average velocity of uniform flow	m/s
U	Liquid velocity component parallel to surface averaged across film thickness	m/s
U_0	Characteristic velocity, (B_0/δ_0)	m/s
v	Velocity in the y-direction	m/s
We	Weber number, $(\rho U_0^2 \delta_0/\sigma)$	
x	Axial coordinate	m

y	Normal coordinate	m
Z	Dimensionless wave celerity, (c/u_0)	

Greek Symbols

Symbol	Definition	Units
α	Wave number, (δ_0/λ)	
δ	Local film thickness	m
δ_0	Mean film thickness over a wavelength	m
ξ_1	Normalized coordinate, $[(\alpha/\delta_0)(x-ct)]$	
ξ_2	Normalized coordinate, (y/δ_0)	
θ	Inclination angle	degree
λ	Wavelength	m
μ	Dynamic viscosity	$kg/m.s$
ν	Kinematic viscosity	m^2/s
ρ	Density	kg/m^3
σ	Surface tension	N/m
τ	Dimensionless time, $(\alpha u_0 t/\delta_0)$	
φ	Dimensionless free surface deflection $(a-1)$	
∇^2	Laplacian operator, $\nabla^2 = \frac{\partial^2}{\partial x^2} + \frac{\partial^2}{\partial y^2}$	

INTRODUCTION

Wavy flow in thin film has been the subject of a large volume of theoretical and experimental investigations.

General method for dealing with the stability of film flow have been applied to set up the main equations of flow (usually the Navier-Stokes equations or the simplified Nusselt equations) on which small perturbations are imposed, leading to an equation of the Orr-Sommerfeld, which can be solved by various approximate methods to determine the conditions of stability^[1,2].

The pioneers researchers in the field of linear stability analyses have shown that a smooth film is unstable for film Reynolds numbers greater than a certain critical value. Kapitsa 1948, who stated that critical Reynolds number for wavy film flow is equal to (5.8).

Yih 1955, applied numerical calculations for stability in case of laminar flow with free surface (neglecting surface tension) of liquid film on a vertical wall.

Hanratty and Hershman 1961 gave an interesting treatment of the stability problem. Hanratty and Hershman stability results were similar to those of the simplified Benjamin theory. Lee^[3] 1969, was the pioneer in non-linear techniques of analysis who carried out, the method of non-linear oscillation to find the amplitudes of the equilibrium waves by seeking for the linear periodic solutions which preserve the periodicity of the actual system when a non-linearity of infinitesimal order is introduced. Esmail^[4] 1980, accounted the profiles of waves traveling over the free surface of a liquid film, falling along an inclined flat wall, using a non-linear technique of dynamic analysis. Lee^[3] 1969, rederived kapitsa's third-order equation for the surface wave motion associated with pseudo-laminar film flow by applying the boundary layer approximation to the Navier-Stokes equation and the free surface conditions. Holgate^[5] 1979, studied experimentally wave development on a thin liquid film, the results were presented for the growth of surface waves on a liquid film that thins as it flows under a gravity over the surface of an

upright circular cone. Hirshburg and Florschuetz^[6] 1982, investigated the hydrodynamic characteristics of thin laminar gravity driven wavy film flow. Brauner and Maron^[7] 1983, studied the modeling of wavy flow in inclined thin films in the absence of interfacial shear. Karapantsios and Karabelas^[8] 1995, used in their experimental examination parallel-wire electrical conductance probe for measuring instantaneous local film thickness to examine dependence of local film characteristics on liquid Reynolds number for vertical pipe location. Mikielewicz and Mikielewicz^[9] (1997), brought in various approaches to modeling a liquid film motion. Karimi and Kawaji^[10] 1999, investigated the flow structure in a thin wavy falling liquid film in a vertical tube with and without interfacial shear induced a counter-current gas flow by using a laser-induced photochromic tracer technique.

EXPERIMENTAL INVESTIGATION:

In order to investigate, the characteristics of wavy falling water film, an experimental setup was constructed. It was designed to allow the measurements of wave profile at different water flow rates and inclination angles. Also, the wavelength and wave velocity can be measured.

The present experimental facility is shown schematically in Fig.(1).

The test channel was mainly designed and constructed in which, visual observation of the flow domain could be made, and the hydrodynamic parameters of the film flow along the channel could be measured. It is assumed reasonably the following goals:

- 1- To allow pivoting of the test channel at different inclination angles.
- 2- To provide convenient access to instrumentation.
- 3- To achieve wavy motion at the free surface of the falling water film.

The test channel was made up of two parts: a water plenum and test section with another separate water plenum, as shown in Fig.(1). The test section is a rectangular channel of 1.78m long, 0.3m wide and 0.1m height. It had its own mechanism, and

permits any inclination between 0° - 90° . The test section and the upper plenum were made from plexi-glass, while the lower plenum was made from metal plate, through which visual observation of the flow field were allowed from all its sides.

For measurement of film thickness, the method of instantaneous thickness measurement using needle contact method is used. This method is based simply of bringing up a needle to the film surface and noting the distance from the wall at which the needle makes contact with the film. Since, there are surface waves on the film in the majority of cases, the needle may touch the film only intermittently. It gives voltage $V(t)$ for an instantaneous liquid film thickness $\delta(t)$. A distribution of the film thickness can be obtained along the channel by measuring the output voltage. Various measuring stations were taken along the test channel to show the variation of film thickness in the flow direction.

The device for the needle contact method consists of a pair of electrodes. One is a tip electrode at the point of an electrically shielded needle, which can be accessed perpendicularly to the flow direction; and the other is a fixed electrode which is touched with the inner surface. The needle was made of stainless wire of (0.5mm) in diameter and a length of (5mm). But the tip of the needle was insulated by painting with a waterproof-insulating adhesive. The needle was glued in a plug, which fixed to a dial gage and a precision micrometer. Direct current with a constant voltage of (5V) is supplied to these two electrodes as shown in Fig.(2) and the current variation due to the difference in resistance of air and water is converted into voltage variation through a load resistance. By precisely measuring (within $\pm 0.01\text{mm}$), the changes in the depth of immersion of the needle in water and the corresponding change of the output voltage, a unique relationship was obtained. Film thickness device calibration was done outside the test section, which permits the use of the device for instantaneous water film thickness during the experimental measurements.

Wave velocity and wavelength measuring process is done using high speed video camera where the time of water entering and exiting along a certain distance is measured for every flow rate and inclination. The process of calculating the time is repeated for several times to check repeatability of measurements.

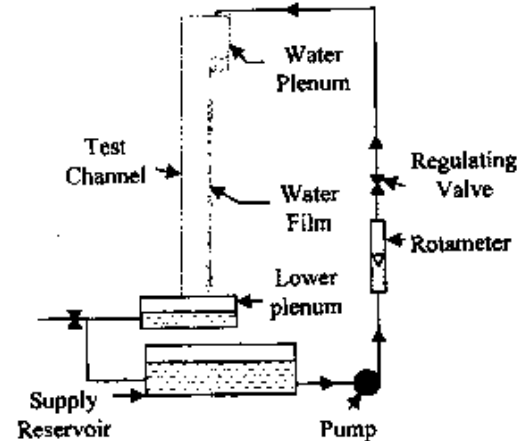


Figure (1) Schematic Diagram of the Experimental Apparatus

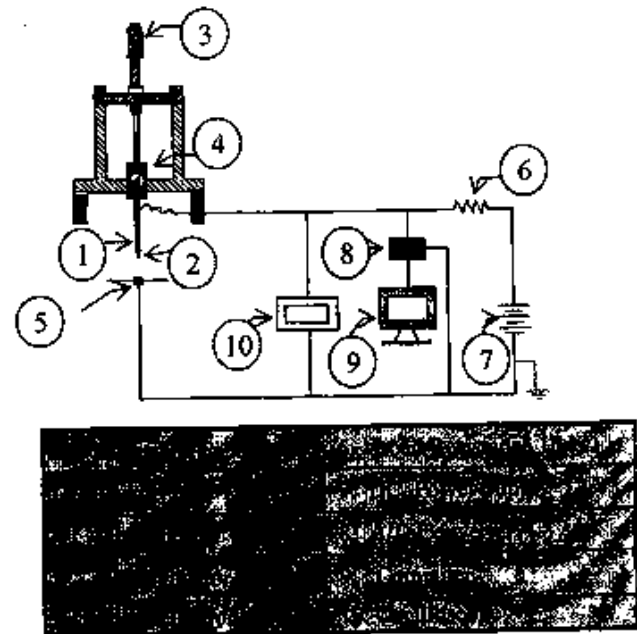


Figure (2) Schematic Diagram of the Film Thickness Measurement System

THEORETICAL ANALYSIS:

A schematic description of falling film is shown in Fig. (3) where water flows along the solid wall. The co-ordinates system for the present model are: the x-axis is directed along the wall, y-axis is taken perpendicular to the wall. The inlet liquid flow rate is \dot{m}_0 . The governing equations, for the present model, are based on the following assumptions:

A . The liquid film flow is considered to be two dimensional periodic wavy flow as the film thickness is small relative to any length scale in the flow direction.

B . The flow of liquid film is laminar and driven by gravity forces only.

C . The liquid is incompressible.

D . The velocity profile is fully developed.

E . The viscous dissipation within the liquid is neglected.

The Mathematical Model:

A thin film of a Newtonian liquid flows down an inclined solid surface at a volumetric flow rate per unit width Q . The flow is taken far enough from the inlet such that it can be considered as fully developed. The general equations for the laminar flow of a viscous incompressible fluid of constant properties, are the Navier-Stokes equations. In terms of the rectangular co-ordinates x, y , these equations may be written as^[6] :

$$\frac{\partial u}{\partial t} + u \frac{\partial u}{\partial x} + v \frac{\partial u}{\partial y} = g_x - \frac{1}{\rho} \frac{\partial p}{\partial x} + \nu \nabla^2 u \quad (1)$$

$$\frac{\partial v}{\partial t} + u \frac{\partial v}{\partial x} + v \frac{\partial v}{\partial y} = g_y - \frac{1}{\rho} \frac{\partial p}{\partial y} + \nu \nabla^2 v \quad (2)$$

The continuity equation given by:

$$\frac{\partial u}{\partial x} + \frac{\partial v}{\partial y} = 0 \quad (3)$$

With the use of the following boundary conditions:

As solid surface $y=0$ for all x

no slip $u=0$

no penetration $v=0$, Thus

$$u=v=0 \quad (4a)$$

At the surface of the liquid at $y = \delta$, the resultant forces are zero, thus

$$e_{ij} n_j t_i = 0 \quad (4b)$$

Which expresses the absence of any applied shear stress at free the surface where:

e_{ij} = Rate of strain tensor

n_j = Unit normal vector at the free surface

t_i = Unit tangential vector at the free surface

Eq. (4b) can be written as, by using strain tensor:

$$\begin{aligned} &\epsilon_{11} n_1 t_1 + \epsilon_{12} n_2 t_1 + \epsilon_{13} n_3 t_1 \\ &+ \epsilon_{21} n_1 t_2 + \epsilon_{22} n_2 t_2 + \epsilon_{23} n_3 t_2 \\ &+ \epsilon_{31} n_1 t_3 + \epsilon_{32} n_2 t_3 \\ &\epsilon_{33} n_3 t_3 = 0 \end{aligned} \quad (4c)$$

$$e_{ij} = 0 \quad \text{for } i \neq j, \quad e_{ij} = 1 \quad \text{for } i=j$$

Therefore, eq. (4c) can be written as:

$$\begin{aligned} &\epsilon_{11} n_1 t_1 + \epsilon_{22} n_2 t_2 + \epsilon_{33} n_3 t_3 = 0 \\ &\text{or} \\ &\frac{\partial u}{\partial x} + \frac{\partial v}{\partial y} + \frac{\partial w}{\partial z} = 0 \end{aligned} \quad (4d)$$

And

$$\begin{aligned} &-(\bar{p} - \bar{p}_v) + 2\mu e_{ij} n_j n_i = \\ &\sigma \left(\frac{1}{R_1} + \frac{1}{R_2} \right) \end{aligned} \quad (4e)$$

in addition, it is convenient to employ a permanent-wave transformation of the form

$$\tau = \frac{\alpha u_c}{\delta_c} t \quad (5)$$

$$\xi_1 = \frac{\alpha}{\delta_c} (x - ct) \quad (6)$$

$$\xi_2 = \frac{y}{\delta_c} \quad (7)$$

Where α is the wave number defined as $\frac{\delta_c}{\lambda}$

c : wave velocity

t : time

The governing differential equations for the asymptotic flow states are then obtained by setting

$\frac{\partial(u)}{\partial \tau} = 0$. The resultant equation are:

$$(\bar{u} - z) \frac{\partial \bar{u}}{\partial \xi_1} + \bar{v} \frac{\partial \bar{u}}{\partial \xi_2} = - \frac{\partial \bar{p}}{\partial \xi_1} + \frac{4}{\alpha \text{Re}} \left[\alpha^2 \frac{\partial^2 \bar{u}}{\partial \xi_1^2} + \frac{\partial^2 \bar{u}}{\partial \xi_2^2} \right] + \frac{Fr}{\alpha} \quad (8)$$

$$\alpha^2 \left[(\bar{u} - z) \frac{\partial \bar{v}}{\partial \xi_1} + \bar{v} \frac{\partial \bar{v}}{\partial \xi_2} \right] = - \frac{\partial \bar{p}}{\partial \xi_2} + \frac{4\alpha}{\text{Re}} \left[\alpha^2 \frac{\partial^2 \bar{v}}{\partial \xi_1^2} + \frac{\partial^2 \bar{v}}{\partial \xi_2^2} \right] \quad (9)$$

Now, turning attention to the boundary condition, (4c) which is specialized to two dimension flow, and by applying continuity equation, this, in normalized form, results in

$$\frac{\partial u}{\partial \xi_2} + \alpha^2 \frac{\partial v}{\partial \xi_1} = \frac{4\alpha^2}{1 - \alpha^2} \frac{\partial a}{\partial \xi_1} \frac{\partial u}{\partial \xi_1} \quad (10a)$$

The same procedure may be applied to(4d) with the aid of(10a), to give

$$P - P_v = - \frac{\alpha^2}{\text{We}} \frac{\partial^2 a}{\partial \xi_1^2} \frac{\partial u}{1 + \alpha^2 a_{11}^2} \quad (10b)$$

Waves on the surface of a thin film are observed to be long waves, consequently, $\lambda \gg \delta_c$ (or $\alpha \ll 1$). Thus, Eq.(8) and(9) can be approximated by:

$$(\bar{u} - z) \frac{\partial \bar{u}}{\partial \xi_1} + \bar{v} \frac{\partial \bar{u}}{\partial \xi_2} = - \frac{\partial \bar{p}}{\partial \xi_1} + \frac{4}{\alpha \text{Re}} \left[\frac{\partial^2 \bar{u}}{\partial \xi_1^2} \right] + \frac{Fr}{\alpha} \quad (11)$$

The boundary equation is similarly scaled. Substituting for the pressure distribution from (10b) in (11) considering that P_v constant yields

$$(\bar{u} - z) \frac{\partial \bar{u}}{\partial \xi_1} + \bar{v} \frac{\partial \bar{u}}{\partial \xi_2} = \frac{\alpha^2}{\text{We}} \frac{\partial^3 a}{\partial \xi_1^3} + \frac{4}{\text{Re}} \left[\frac{\partial^2 \bar{u}}{\partial \xi_1^2} \right] + \frac{Fr}{\alpha} \quad (12)$$

Eq. (12) can be simplified further via an appropriate assumption for the y-dependence of velocity field. the most frequently assumed distribution is the parabolic profile:

$$u = Ay^2 + By + C \quad (13)$$

Applying the B. C:

$$u=0 \text{ at } y=0 \quad (14a)$$

$$u = \frac{3}{2} U \text{ at } x = \delta \quad (14b)$$

$$U = \frac{1}{\delta} \int_0^{\delta} u dy \quad (14c)$$

substitution B. C from eq. (14) in eq. (13) yield:

$$u = 3b \left[\frac{\xi_2}{a} - \frac{\xi_2^2}{2a^2} \right] \quad (15)$$

where

$$\xi_2 = \frac{y}{\delta}$$

from the continuity eq.(3) the velocity in y-direction can be obtained as:

$$v = - \int_0^y \frac{\partial u}{\partial x} dy \quad (16)$$

Using eq.(15) in eq(16) gives:

$$v = 3 \frac{db}{d\xi_1} \left(\frac{\xi_1}{a} - \frac{\xi_2^2}{2a} \right) + 3a \left(\frac{\xi_2^2}{a^3} \frac{da}{d\xi_1} - \frac{\xi_2}{a^2} \frac{da}{d\xi_1} \right) \quad (17)$$

Now, substituting for the velocity in the x- and y-directions into eq.(12) gives:

$$\begin{aligned} & \frac{\alpha^2}{We} a^3 \frac{d^3 a}{d\xi_1^3} + (za^2 - \frac{9}{10} ab) \frac{db}{d\xi_2} \\ & + \left(\frac{6}{5} b^2 - \frac{3}{2} zab \right) \frac{da}{d\xi_1} - \frac{12}{\alpha Re} b \\ & + \frac{Fr}{a} a^3 = 0 \end{aligned} \quad (18)$$

The film flow rate could be related to the local film thickness by integration of the continuity equation over the film thickness. The surface kinematics relation which may be written in dimensionless form as^[6]:

$$\frac{d}{d\xi_1} (b - za) = 0 \quad (19)$$

Integrating and averaging over a wavelength to find the constant of integration yield:

$$b = z\phi + l \quad (20)$$

Where (a) has been replaced in favor of the dimensionless deflection of the free surface from its mean location. i.e.

$$(21)$$

$$\phi = a - l$$

Using (20) and (21) in (18) yield the following equation of free surface deflection:

$$\begin{aligned} & \frac{\alpha^2}{We} (1 + \phi)^3 \phi''' + \frac{\alpha}{5} [(5z^2 - 12z + 6) \\ & - z^2 \phi (2 + \phi)] \phi' + Fr \phi^2 (3 + \phi) \\ & + (3Fr - \frac{12z}{Re}) \phi + (Fr - \frac{12}{Re}) = 0 \end{aligned} \quad (22)$$

This equation describe the profile of the freely falling film along the axis of the flow direction. It can be solved numerically using *Runge-Kutta* method.

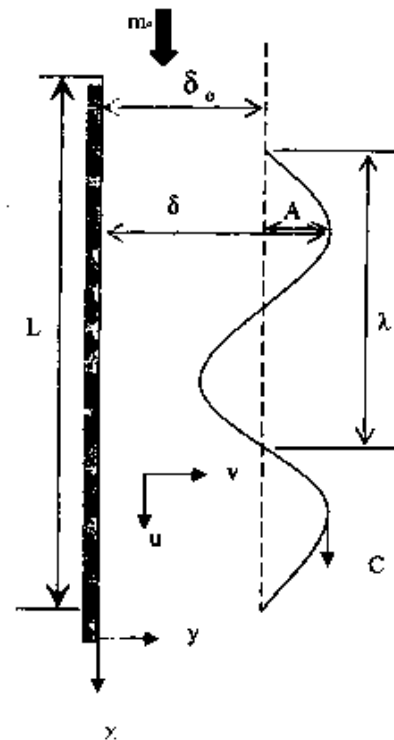


Figure (3) Schematic Description of the Physical Model and Coordinates

RESULTS AND DISCUSSION:

Figure (4) shows the variation of water film thickness with time at a flow rate of $0.3 \text{ (m}^3/\text{h)}$, at a position of measurement point of (0.2m) distance from the entrance at an inclination angle of 80° . While in figure (5) shows the variation of water film at $0.4 \text{ (m}^3/\text{h)}$ at the same position distance, i.e. (0.2m) and inclination angle.

In these two figures, the water profile is fluctuating and in some where is of harmonic shape. Careful inspection of the experimental signals reveals that the substrate is covered by excessively dense disturbances of very low amplitude. These small disturbances are capillary waves and represent a salient feature of falling film surface. Figures (6 and 7), show the variation of water film thickness with time at the flow rates $0.3 \text{ (m}^3/\text{h)}$ and $0.4 \text{ (m}^3/\text{h)}$ respectively but a position (0.8 m) from entrance. Average film thickness and also wave deformation increase with flow direction. Figures (8 and 9), illustrate the variation of water film thickness with time at $0.3 \text{ (m}^3/\text{h)}$ and $0.4 \text{ (m}^3/\text{h)}$, at (1.6 m) distance from entrance at an inclination angle of 70° . Deformation of the wave also increases because of the long distance and irregular waves appearance at the down stream of the channel. Figures (10, 11, 12, 13, 14 and 15), show the variation of film thickness with time at $(0.3 \text{ and } 0.4) \text{ (m}^3/\text{h)}$ at distances $(0.2, 0.8, \text{ and } 1.6\text{m})$ respectively. It is concluded that the average film thickness increases with increasing the distances of entrance position besides increasing the wave deformation because of the high wave velocity. Figure (16), illustrate the variation of average film thickness with water flow rate for different measurement positions. The average film thickness increases with increasing water flow rate, but with different increment at the various measurement locations. Figure (17), shows the theoretical wave velocity which agrees well the measured wave velocity prediction for different Re number. Figure (18) shows a comparison the wave profile of theoretically predicted from the mathematical model with that obtained from the experimental results. Fair agreement is obtained which proves

the validity of the theoretical model. Figure (19) shows the comparison between theoretical and experimental results of the dimensionless wave celerity with Re numbers at an 80° degree angle of inclination. Wave celerity increased with increasing Re number. Figure (20) shows a comparison between theoretical and experimental results of the wave velocity with Re numbers at 80° degree angle of inclination. This figure illustrates that the good agreement between the Theoretical and the Present work with Takahama and Kato⁽¹¹⁾ wave velocity increase with increasing Re numbers. Figure (21) shows a comparison between the experimental results of the wavelength for the water film thickness at the 80° degree inclination angle. This figure shows that with increasing the flow rate, wavelength decreases as a result of increasing wave velocity. Fair agreement is obtained between the present work and that of Hirsburg and Florschuetz⁽⁶⁾.

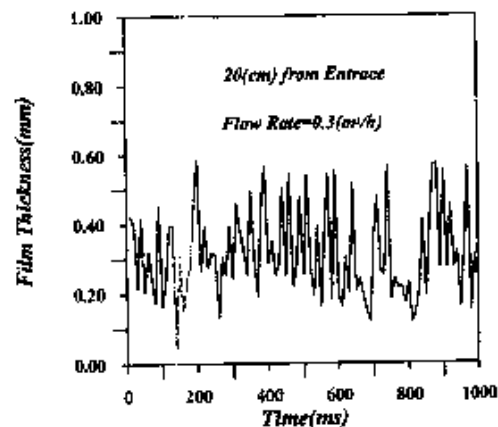


Fig.(4) Variation of Film thickness with time at flow rate $0.3 \text{ (m}^3/\text{h)}$, Inclination = 80°

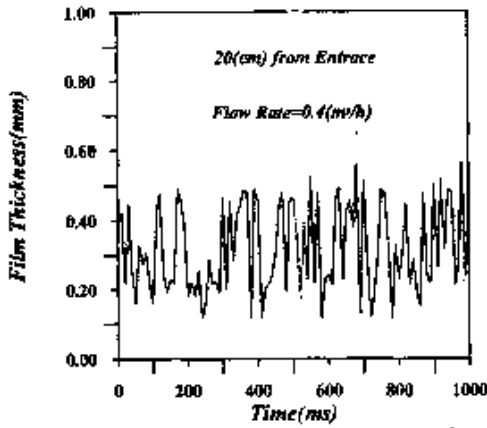


Fig.(5) Variation of Film thickness with time at flow rate 0.4(m³/h), Inclination = 80°

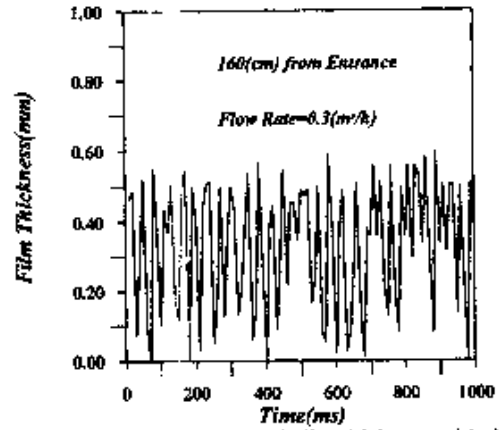


Fig.(8) Variation of Film thickness with time at flow rate 0.3 (m³/h), Inclination = 80°

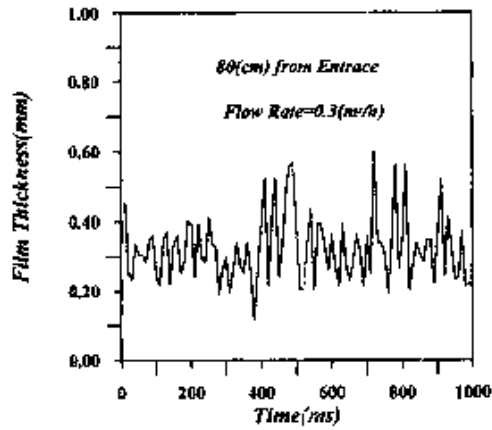


Fig.(6) Variation of Film thickness with time at flow rate 0.3 (m³/h), inclination = 80°

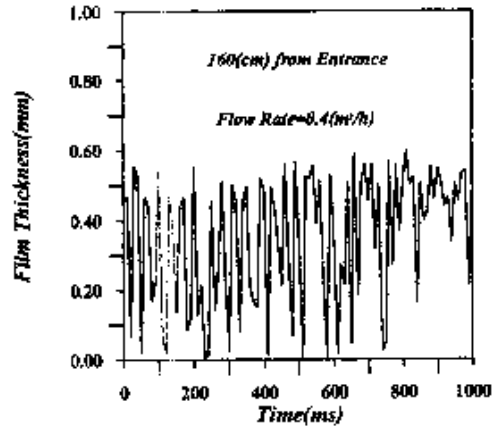


Fig.(9) Variation of Film thickness with time at flow rate 0.4(m³/h), Inclination = 80°

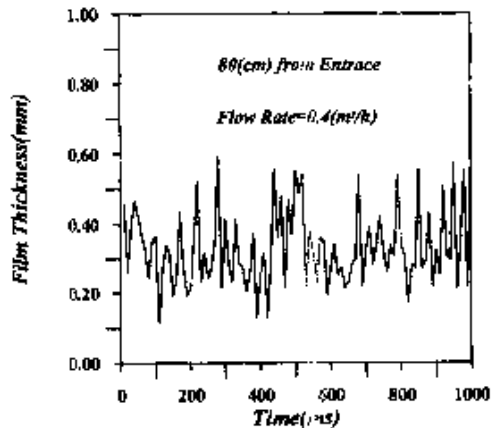


Fig.(7) Variation of Film thickness with time at flow rate 0.4(m³/h), Inclination = 80°

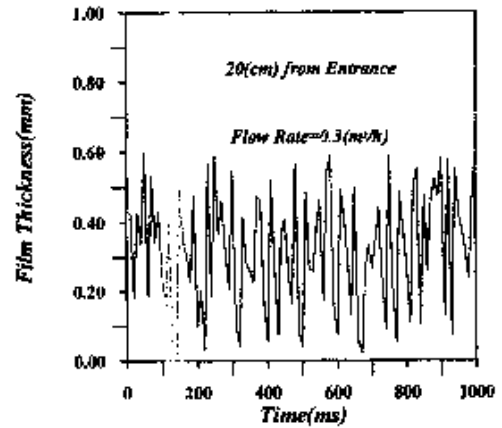


Fig.(10) Variation of Film thickness with time at flow rate 0.3(m³/h), Inclination = 70°

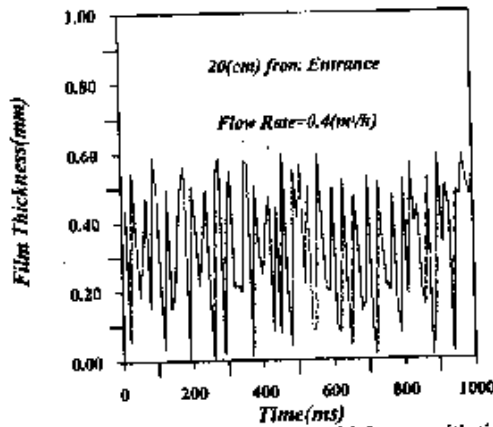


Fig.(11) Variation of Film thickness with time at flow rate 0.4(m³/h). Inclination = 70°

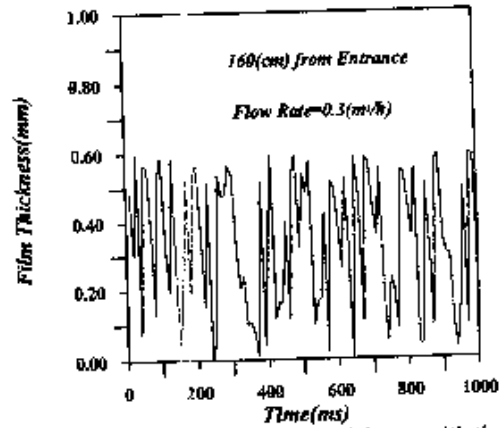


Fig.(14) Variation of Film thickness with time at flow rate 0.3(m³/h). Inclination = 70°

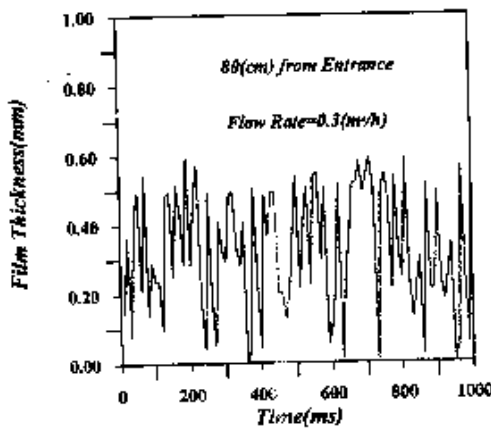


Fig.(12) Variation of Film thickness with time at flow rate 0.3(m³/h). Inclination = 70°

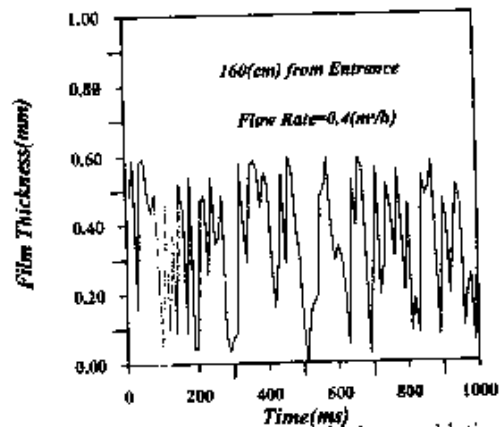


Fig.(15) Variation of Film thickness with time at flow rate 0.4(m³/h). Inclination = 70°

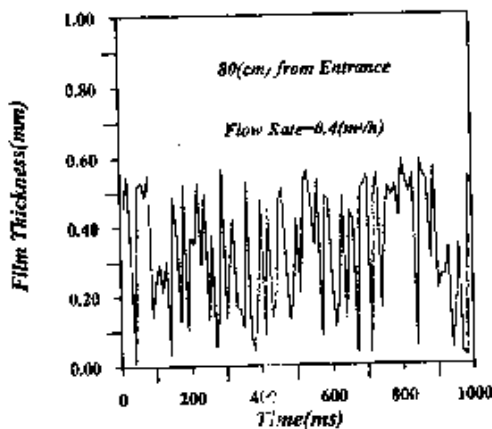


Fig.(13) Variation of Film thickness with time at flow rate 0.4(m³/h). Inclination = 70°

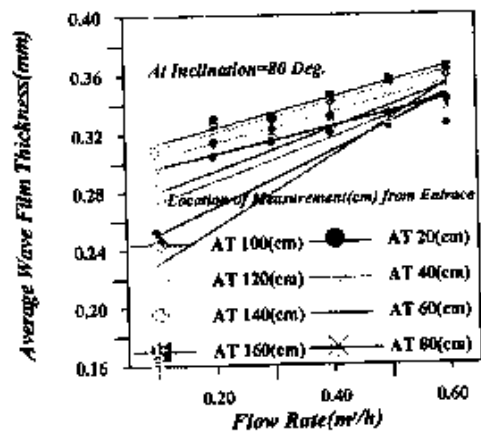


Fig.(16) Variation of the flow rate with average wave film thickness at 80° angle of inclination.

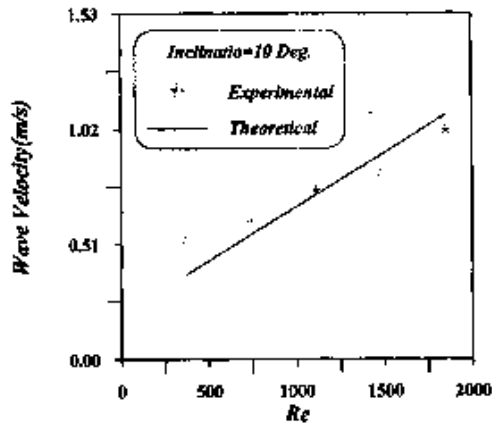


Fig. (17) Comparison between the Reynolds Number with the theoretical and experimental velocity values at inclination = 10°.

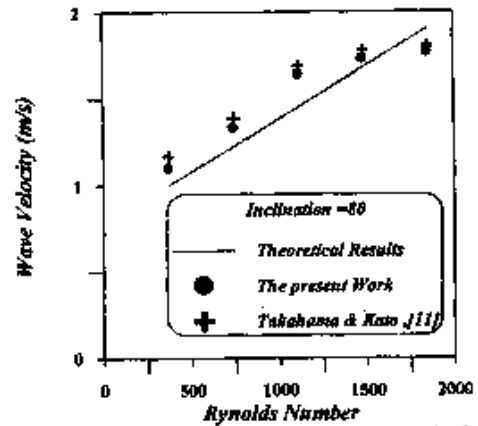


Fig. (20) Comparison between Wave Velocity and Reynolds Number, theoretical and experimental, at inclination angle = 80°.

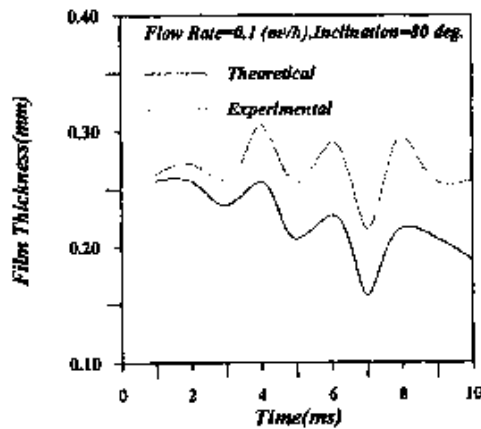


Fig. (18) Comparison between theoretical and experimental results of the film thickness at flow rate = 100 (m³/h), inclination angle = 80°.

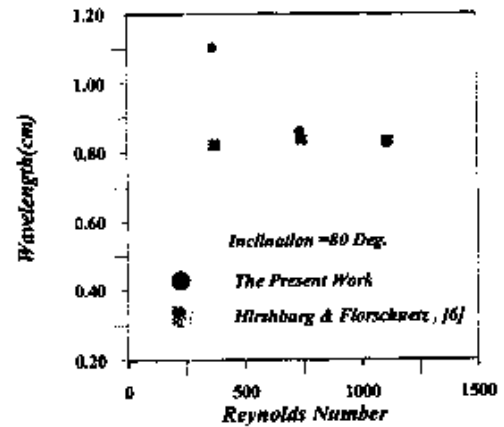


Fig. (21) Comparison between Wavelength and Reynolds Number, theoretical and experimental, at inclination angle = 80°.

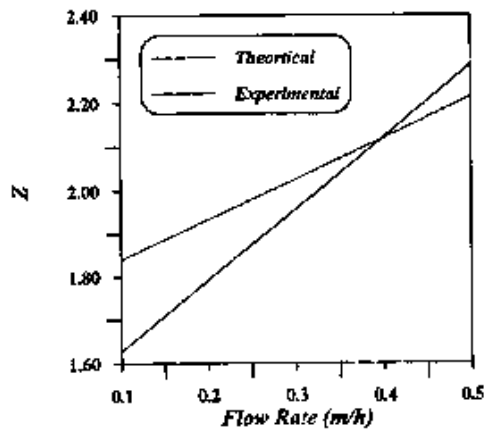


Fig. (19) Comparison between Celerity wave and flow rate, theoretical and experimental, at inclination angle = 80°.

CONCLUSIONS:

Experimental characteristics of falling water film was investigated for different water flow rate, inclination angles at different measuring stations along the flow line. The experimental signals were analyzed and the wave profile showed to be fluctuating and of harmonic trend with substrate covered by extensively dense disturbances of very low amplitude. The average wave thickness increased with both flow rate and location. The mathematical prediction of the wave profile agreed well with the experimental results, which proves the validity of the present model. Beside the wave profile, the wave velocity and wavelength measurements agreed fairly with the theoretical prediction and with the results of previous investigations.

References:

- [1] Fulford, G.D. "The Flow of Liquid in Thin Film", *Advances in Chemical Engineering*, vol. 15, pp. 151-229, 1964.
- [2] AL-Salman, K. Y., "Analysis of Direct Contact Condensation on Subcooled Wavy Falling Liquid Film", Ph. D, Thesis, University of Basra, College of Engineering, Mechanical Department, 2002.
- [3] Lee, Y. "Kapitza's Method of Film Flow Description", *Chemical Engineering Science*, vol. 24, pp. 1309-1319, 1969.
- [4] Esmail, M. N., "Wave Profiles on Inclined Falling Film", *The Canadian J. Chem. Eng.*, Vol. 58, pp. 145-150, 1980.

[5] Holgate, M. J., "Wave Development on a Thinning Liquid Film", *Int. J. Heat & Fluid Flow*, vol. 1, No. 1, pp. 17-24, 1979.

[6] Hirshburg, R. I. and Florschuetz, L. W. "Laminar Wavy Film Flow: Part II, Condensation and Evaporation", *J. of Heat Transfer*, vol. 104, pp. 459-464, 1982.

[7] Brauner, N., and Maron, D.M., "Modeling of Wavy Flow in Inclined Thin Films", *Chem. Eng. Science*, Vol. 38, No. 5, pp. 775-788, 1983.

[8] Karapanisios, T. D. and Karabelas, A. J., "Longitudinal Characteristics of Wavy Falling Films", *Int. J. Multiphase Flow*, Vol. 21, No. 1, pp. 119-127, 1995.

[9] Mikielwicz, J. and Mikielwicz, D. "Modeling of Wavy Liquid Film Flow" *Archives of Thermodynamics*, vol. 17, pp. 81-108, 1996.

[10] Karimi, G. and Kawaji, M. "Flow Characteristics and Circulatory Motion in Wavy Falling Films with and without Counter-current Gas Flow", *Int. J. Multiphase Flow*, Vol. 25, pp. 1305-1319, 1999.

[11] Takahara H., and Kato, S., "Longitudinal Flow Characteristics of Vertically Falling Liquid Films without Concurrent Gas Flow", *Int. J. Multiphase Flow*, Vol. 6, pp. 203-215, 1980.